COLOUR CENTRES DEVELOPMENT BY GAMMA-IRRADIATION OF NATURAL AND SYNTHETIC ROCK SALT SAMPLES

C.de las Cuevas, L.Miralles

ABSTRACT

Laboratory gamma irradiations at a constant temperature (100ºC) were carried out in four sets of experiments. The starting materials for the experiments were both natural and synthetic rock salt. Dose rates were approximately constant for two of the experiments and variable for the other two. The total doses studied ranged from 20 kGy to 1154 MGy. Measurements of the concentration of colour centres (radiation induced defects) were performed using two methods: optical absorption and release of hydrogen after dissolution of irradiated salt. The results were compared with the dose absorbed, dose rate and chemical composition of the rock salt. The concentration of colour centres increases with increasing total dose, being lower dose rates slightly efficient in the generation of colour centres for samples irradiated at the same total dose. The mineralogical composition of the rock salt also affects the concentration of the defects, leading to a dispersion of one order of magnitude. In these experiments, mineralogical composition had more influence than dose rate in generating radiation-induced defects. The process of fluid-assisted recrystallization in the form of newly precipitated white halite was extensive in pure polycrystalline rock salt (natural and synthetic). These crystals, which precipitated after irradiation, included equivalent amounts of H_2 to the concentration of colloidal sodium developed in the damaged crystals. Comparison between experimental data and the Jain-Lidiard model predictions performed in the range of 20 kGy and 50 MGy, revealed that for doses higher than 5 MGy the model is a good aproximation.

1. INTRODUCTION

The disposal of high-level radioactive waste in rock salt can lead to a series of changes of state in the surrounding rock salt. The radiation emitted by radioactive waste canisters will be absorbed by the salt formation in the course of time. Most of the gamma radiation energy will be converted into heat, whilst a small part will induce radiation damage. This consists of the generation of defects in the crystal lattice of the halite (NaCl) which is the major mineral in rock salt (over 90 %). Although only the first meter in contact with the

wastes will be affected (Schulze, 1986), this phenomenon needs to be studied carefully in order to ensure that it will not threaten the long-term safety of the repository.

When sodium chloride is irradiated, the primary defects generated are pairs of F and H- centres. Cl^- ions are ejected from their normal lattice sites to form interstitial chlorine atoms (H-centres). The former structural site of chloride traps an electron (F-centre), and the neutrality of the crystal is preserved. At temperatures above 30ºC, as is the case of heat-producing waste, the mobility of primary defects is increased (Hodgson *et al.*, 1979). Due to their high mobility the H-centres (activation energy about 0.1 eV) are easily trapped in the vicinity of dislocation lines, where molecular chlorine is formed, and the F-centres, which are less mobile (activation energy about 0.8 eV), tend to form clusters of two or more centres (e.g. M-, R-centres). Because of their optical properties, they all absorb light in the visible range of the electromagnetic spectrum (F, M, R and other centres), and are thus referred to as colour centres. If the clustering continues, larger aggregates of metallic sodium colloids are formed. The theory which describes the growth of the sodium colloids by irradiation of NaCl crystals was advanced by Jain and Lidiard (1977).

Radiation damage in halite has been extensively studied for low doses by several authors in the field of Solid State Physics (Przibram, 1956; Dale Compton, 1957). Over the last twenty years, its study has been extended to high doses (Jenks and Bopp, 1974; Levy, 1983) since a sudden recombination of the defects accumulated could constitute a possible hazard related to the radiation damage in salt repositories. As a consequence, the local temperature would rise around the emplacement of wastes (Mönig *et al.*, 1990)

In natural rock salt, there are large variations in the radiation damage as it depends on: temperature, the level of impurities, dose rate, total dose and strain on the rock sample (Levy, 1983). In addition, fluid-assisted recrystallization (García Celma *et al.* 1988) may take place, annealing the damage of the rock salt. For these reasons, a study of radiation damage in natural rock salt from several locations and in synthetic rock salt has been undertaken. Four sets of experiments were carried out at two Gamma-Irradiation Facilities (GIF A and GIF B) located at the cooling pool of the High Flux Reactor (Petten, The Netherlands), in which spent fuel elements are used as source of gamma radiation (article 5 in this volume).

2. EXPERIMENTAL PROCEDURE

Samples for the GIF A-1 experiment were irradiated at 100 ºC and atmospheric pressure. Dose rate was variable (between 200 and 20 kGy/h) and total doses ranged from 41 to 1223 MGy. Samples for the GIF A-2 experiment were irradiated at atmospheric pressure at a temperature that varied from 130 ºC at the beginning of the irradiation to 100 ºC after three days. Dose rate was variable (between 170 and 40 kGy/h) and total doses ranged from 19 to 48 MGy. The starting material used in the experiments was SP800 rock salt from the Asse Mine (Remlingen, Germany) for the GIF A-1 experiment, and rock salt from the Sallent Mine (Barcelona, Spain) for the GIF A-2 experiment.

The starting material for the GIF B-1 and GIF B-2 experiments were cores of both natural and synthetic rock salt. Samples of natural rock salt came from the Sallent Mine (Barcelona, Spain) at level 323 (coded PLL), from the Asse Mine (Remlingen, Germany) (coded SP800, Bha , Bhp or PS depending on stratigraphical position) and from Dutch salt formations (coded DS). Synthetic polycrystalline rock salt was obtained from an analytical NaCl reagent, and was divided into two types (coded PP, which is a fine grained rock salt, or SS, which is a coarse grained rock salt). Finally, pure monocrystals (manufactured by Harshaw Chemical Co., Ohio, USA; coded H) are also used. Samples were turned on a lathe until they reached a diameter of 24 mm and then cut to form cylinders (40 mm length) and tablets (10 mm length). Irradiations from the GIF B-1 experiment were performed at an approximately constant dose rate of 15 kGy/h (which ranged from 20 to 10 kGy/h) and the temperature during irradiation was kept constant at 100ºC. Total doses ranged from 20 kGy to 44 MGy. In each loading, 8 containers (6 of them pressurized at 20 MPa in order to simulate the confining pressure at depths of 800 m and the other two at atmospheric pressure) were irradiated simultaneously. Every container had inside a cylinder and a tablet shaped sample. The experimental conditions for the GIF B-2 experiment were identical to those of the GIF B-1 except that the dose rate was around 4 kGy/h.

The quantification of the fraction of the radiation-induced defects present in the NaCl lattice was performed by optical absorption measurement on translucent thin sections, 30 to 250 µm thick, depending on its opacity. Low-speed procedures were applied to obtain the thin sections in order to avoid damage induced by sample manipulation. Optical Absorption measurements (O.A) were performed using a double beam UV-Vis spectrophotometer. The spectral interval scanned was from 300 to 900 nm (Fig. 1), since F-centres show an absorption band at about 460 nm, M-centres at 700 nm, and the sodium colloids between 550 and 650 nm. In the case of halite containing impurities in its crystal lattice (Ikeda and Yoshida, 1967), F-centres are absent, being F_A or F_Z centres present (F-centres developed in

the vicinity of either a monovalent or a divalent cation impurity). These F-related centres show an absorption band between 380 and 420 nm. These bands commonly overlap and, in order to obtain better resolution, the spectra must be deconvolved (Fig. 2) using a Fast Fourier Transform filter. Afterwards, the concentration of colour centres was quantified from the absorbance of each band using Smakula's equations (1) (Markham, 1966) and (2) (Levy and Kiersted, 1984), which relate the absorption coefficient to the concentration of colour centres.

$$N = \alpha_{max} \frac{10^{16}}{2.06\, f} \qquad (1) \qquad \text{(for F-centres)}$$

$$FM = 4.42\ 10^{-7}\ \alpha_{max} \qquad (2) \qquad \text{(for colloidal sodium)}$$

where α_{max} is the maximal absorption coefficient in cm^{-1}
f, the oscillator strength (between 0.8 and 0.9)
N is the number of F-centres per cm^3
FM is the molar fraction of colloidal Na.

The absorption coefficient is computed by the equation (3)

$$\alpha = \frac{\ln 10}{t} Abs \qquad (3)$$

where α is the absorption coefficient in cm^{-1}
t is the thickness of the sample in cm
Abs is the absorbance

Besides the concentration of colour centres, additional information can be obtained from the absorption spectra, such as the size of the colloids (Smithard and Tran, 1974) which can be related to the exact location of the optical absorption peak and/or to its width.

Moreover, quantification of sodium colloids by measuring the release of hydrogen during dissolution of irradiated salt samples (Jenks *et al.*, 1975) was also carried out, in order to contrast the aforementioned methodology. Grounded salt amounting 500 mg were dissolved in 1.5 ml of distilled water in a glass vial (V= 5 ml) which was closed with an

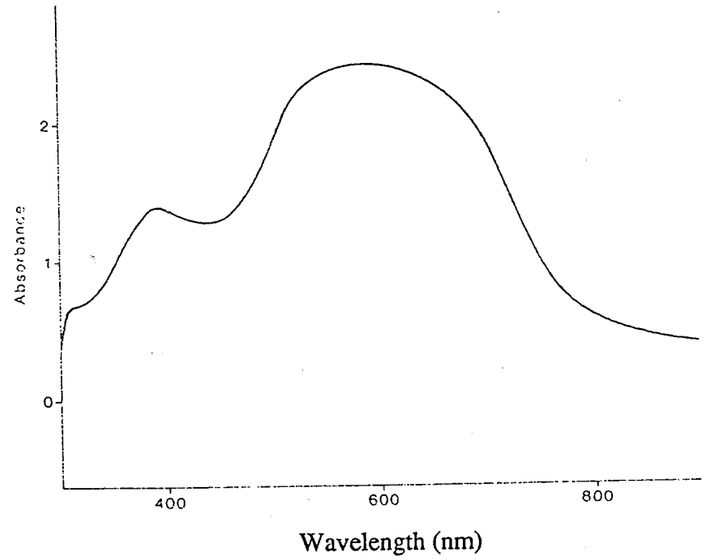

Figure 1: Absorbance spectrum of sample 1PLL.

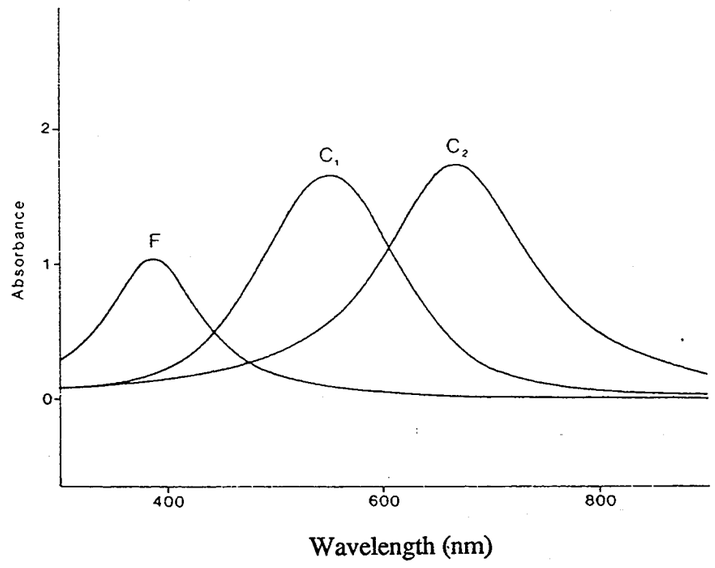

Figure 2: Deconvolved absorbance spectrum of sample 1PLL showing the presence of F-related centres and two populations of colloidal sodium particles.

open-hole screw-cap and a septum. The evolved hydrogen produced by the reaction of metallic sodium with water, was extracted via a gastight syringe and measured by gas chromatography. The working conditions were: Molecular Sieve column, Thermal Conductivity Detector, Argon as carrier gas and oven temperature hold to 60°C.

Geochemical characterization was performed only on the cylindrical samples from the GIF B-1 and GIF B-2 experiments. After crushing to a grain size of 2 to 3 mm, 250 mg was taken for water content analysis and quantified by thermogravimetry. In natural rock salt samples 5 to 10 g of the crushed material were further milled, and chemical and mineralogical analyses were performed. Chloride was determined volumetrically, sulphate by ICP-AES (Inductively Coupled Plasma Atomic Emission Spectroscopy), potassium by AES (Atomic Emission Spectroscopy) and calcium, magnesium and strontium by AAS (Atomic Absorption Spectroscopy). The insoluble fraction was calculated gravimetrically. The analytical procedures are described in detail elsewhere (Huertas *et al.*, 1992).

The mineralogical phases present in the irradiated rock salt from the GIF B-1 and GIF B-2 experiments were identified with a transmitted-light polarizing microscope in the aforementioned thin sections. The microscope study of thin sections also revealed microstructural changes in the starting material and permitted quantification of the damage-free halite precipitated in the experiments. The quantification was performed using an automated image analyzer.

3. RESULTS

3.1 Defect concentration in samples from the GIF A-1 experiment

F-related centres were quantified for all the samples of the GIF A-1 experiment from Optical Absorption spectra. Their concentrations ranged from $3.25 * 10^{-5}$ to $3.74 * 10^{-4}$ molar fraction. The colloidal sodium concentration of samples irradiated at doses of 41 and 86 MGy could be measured by O.A and release of hydrogen, both of which gave similar values. The amount of colloidal sodium ranged from $2.0* 10^{-4}$ to $6.0* 10^{-4}$ molar fraction. Moreover, two size of colloids (around 2 and 100 nm) could be determined. At higher doses (150 MGy and above), the O.A spectra of these samples are very complex to study, due to the high dose absorbed. For this reason the concentration of colloidal sodium was computed from the release of hydrogen from dissolved samples. The concentration of colloidal sodium ranged from $1.3* 10^{-3}$ to $4.9*10^{-3}$ molar fraction. The broad O.A band related to colloidal

sodium has been interpreted as the result of concentration of metallic sodium particles greater than $1* 10^{-3}$ molar fraction, with size ranging from 2 to 150 nm.

3.2 Defect concentration in samples from the GIF A-2 experiment

The irradiation experiment of GIF A-2 was performed with a similar dose rate to the GIF A-1 experiment but covering a lower dose region (between 19 and 50 MGy). In the samples studied, F-related centres, and one or two sizes of colloidal sodium particles (depending on the sample) were detected by O.A. The size of colloidal particles varied from 45 to 90 nm diameter. When the size of the colloids was around 90 nm, a second population of small size colloids was present (diameter between 1 and 50 nm). There is good correlation in the colloidal sodium measurements between Optical Absorption and evolved hydrogen methods, which give results of the same order of magnitude. The concentration of colloidal sodium was between $7.6 * 10^{-5}$ and $6.3 * 10^{-4}$ molar fraction and that of F-related centre was between $4.1 * 10^{-6}$ and $6.6 * 10^{-5}$ molar fraction.

The concentration of F-centres and colloids obtained in both variable dose experiments (GIF A-1 and GIF A-2) are plotted versus the total dose in Figures 3 and 4. A linearity of the amount of radiation induced defects in the range between 19 and 300 MGy is observed. Nevertheless, at higher doses there is a change in the slope suggesting decreasing efficiency in generating defects.

3.3 Defect concentration in samples from the GIF B-1 experiment

F- or F-related centres and sodium particles of colloidal size were found in all the samples. F-centres were present only in pure monocrystals, whereas F-related centres (F_A or F_Z centres) were found in polycrystalline rock salt. Moreover, M-centres were detected mainly in pure monocrystals, at concentration below 10^{-6} molar fraction. For doses below 430 kGy, the concentration of colloidal sodium is only measurable using the evolved hydrogen method since from the O.A spectra only F-centres could be quantified. At higher doses (430 kGy and above) colloidal sodium could also be measured from the O.A spectra. There is good correlation in the colloidal sodium measurements between both methods, Optical Absorption and evolved hydrogen, yielding results on the same order of magnitude. The amount of colloidal sodium, which increases with total dose, ranged between less than 10^{-7} to $5.25 * 10^{-4}$ molar fraction for doses of 48 MGy. The concentration of F-centre does not increase sensitively with total dose and ranged between $1.5* 10^{-6}$ to $1.0 * 10^{-4}$ molar

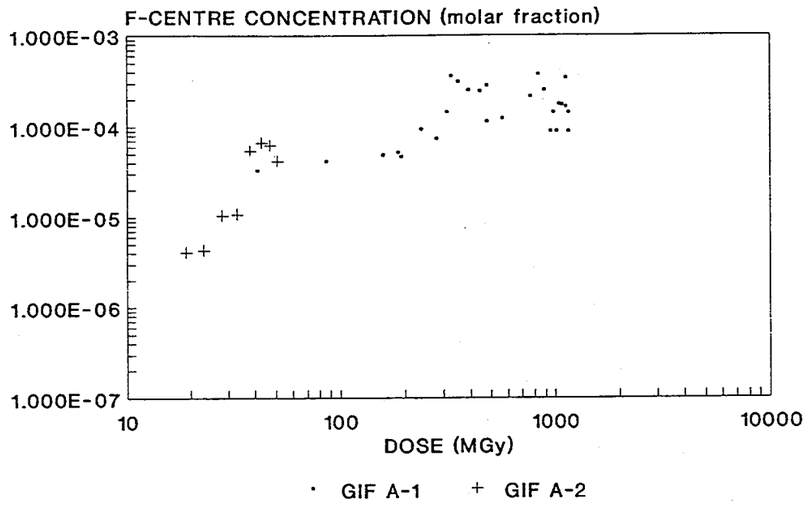

Figure 3: F-centre concentration versus total dose for samples from GIF A-1 and GIF A-2 experiments.

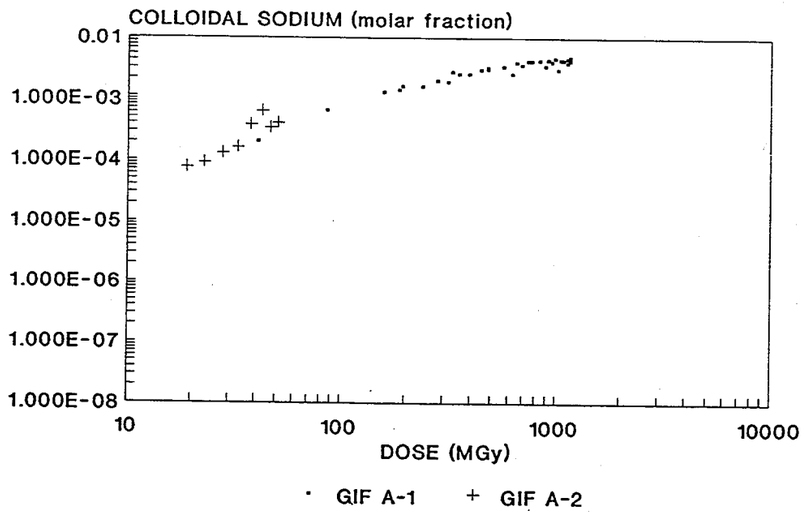

Figure 4: Colloidal sodium concentration versus total dose for samples from GIF A-1 and GIF A-2 experiments.

fraction. The concentration of the radiation induced defects are displayed in figures 5 and 6. Figure 5 shows the relationship between total dose and the amount of F- or F related centres. Figure 6 shows the relationship between total dose and the amount of colloidal sodium. For samples of the same type and irradiation conditions, the amount of defects varied widely, suggesting a substantial contribution of the geological parameters of the starting material. It has been observed that for the same total dose pure monocrystals developed less colloidal sodium (about one order of magnitude) than polycrystalline rock salt.

For polycrystalline rock salt the size of the colloidal particles usually grows with increasing total dose. Nevertheless, in several samples irradiated at doses higher than 16 MGy in addition to the colloidal sodium particles about 90 nm diameter, a second population of colloids of smaller size (about 5 nm diameter) was also present. In pure monocrystals, the size of the colloidal particles was always around 90 nm diameter, indepently on their concentration. In figure 7 the relationship between total dose and the size of the colloidal particles is plotted.

3.4 Defect concentration in samples from the GIF B-2 experiment

In all the samples F- or F-related centres and a population of colloidal sodium were present. In addition, in samples irradiated at doses higher than 10 MGy, a second population of colloidal sodium was detected in natural rock salt. In contrast for Pressed Powder samples and pure monocrystals, M-centres were normally found. The two population of colloids present in natural rock salt have been divided as small sized (between 1 and 60 nm diameter) and big sized (between 80 and 90 nm diameter). As in samples from the GIF A-2 and GIF B-1 experiments, there is also good correlation in the colloidal sodium measurements between Optical Absorption and evolved hydrogen methods.

The total amount of colloidal sodium particles ranged from $3 * 10^{-7}$ to $8.23 * 10^{-4}$ molar fraction, the amount of F-related centre ranges from $6 * 10^{-7}$ to $9.6 * 10^{-5}$ molar fraction and the amount of M-centre (when detected) ranged from 10^{-7} to $5.26 * 10^{-4}$ molar fraction. There is an increase of the amount of defects with increasing dose. Moreover, the size of the colloidal particles grows with increasing dose.

The behaviour of the radiation induced defects in these samples is similar to their equivalents of the GIF B-1 experiment. Figure 8 shows the relationship between total dose and the amount of F- or F related centres. Figure 9 shows the relationship between total dose and the amount of colloidal sodium particles, whereas in figure 10 the relationship between

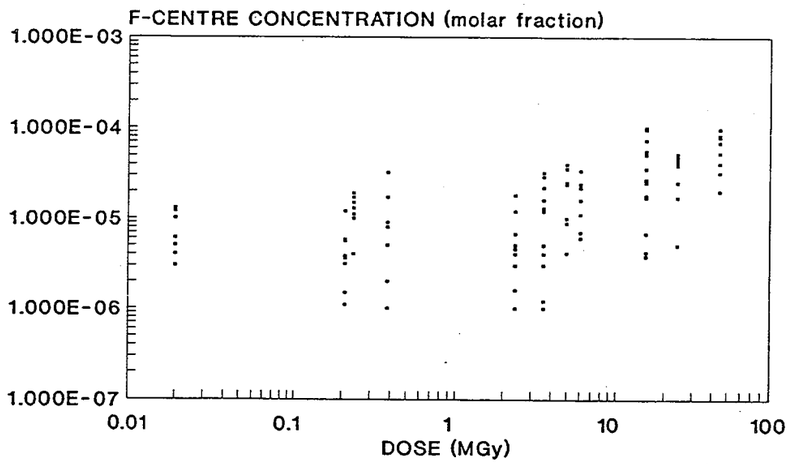

Figure 5: F-centre concentration versus total dose for samples from GIF B-1 experiment.

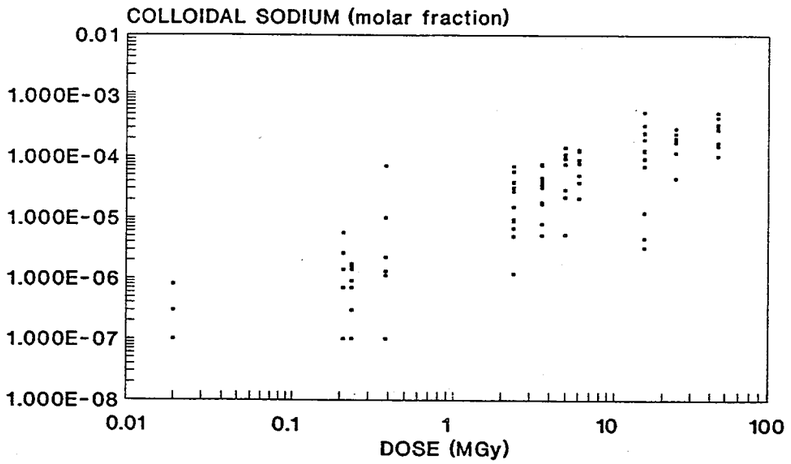

Figure 6: Colloidal sodium concentration versus total dose for samples from GIF B-1 experiment.

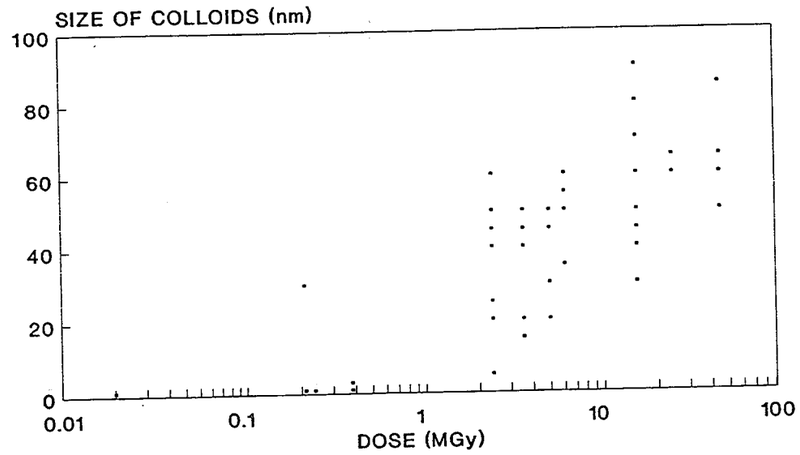

Figure 7: Size of colloidal sodium particles versus total dose for samples from GIF B-1 experiment.

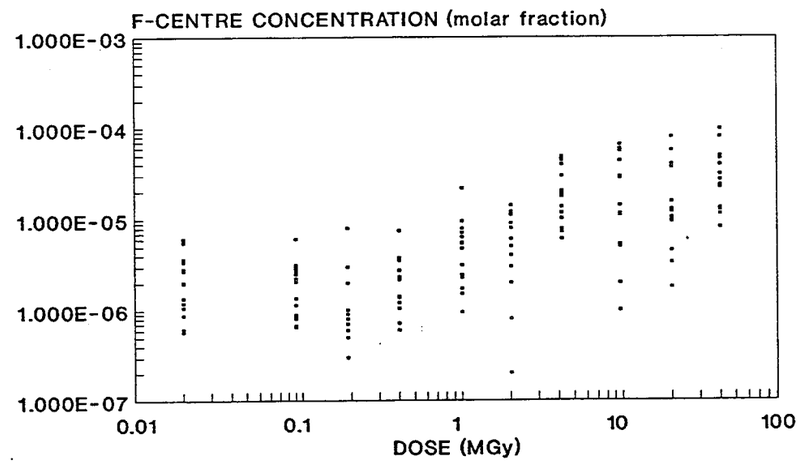

Figure 8: F-centre concentration versus total dose for samples from GIF B-2 experiment.

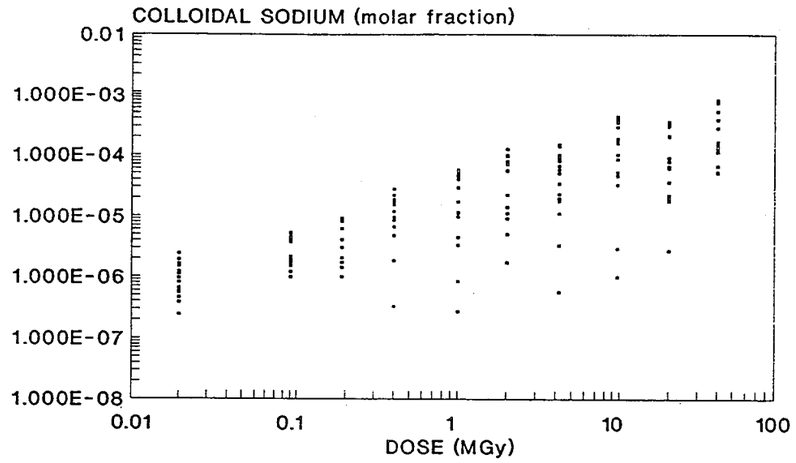

Figure 9: Colloidal sodium concentration versus total dose for samples from GIF B-2 experiment.

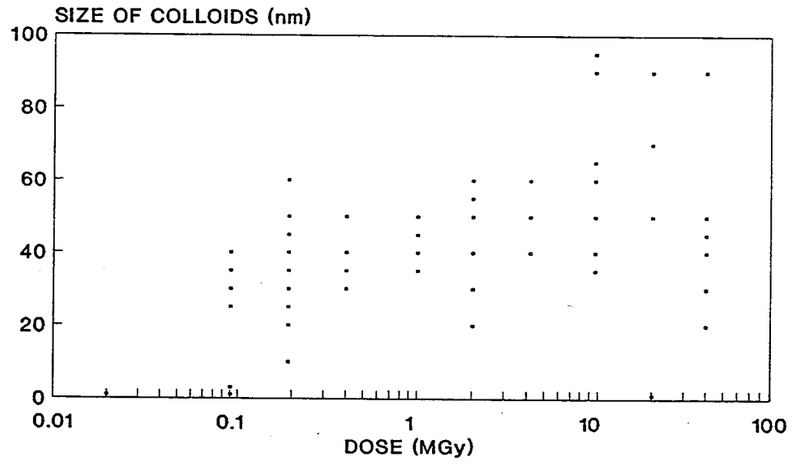

Figure 10: Size of colloidal sodium particles versus total dose for samples from GIF B-2 experiment.

total dose and the size of the colloidal particles is plotted.

It has been postulated by Van Opbroek and den Hartog (1985) that lower dose rates are more efficient in generating defects. Comparing absolute amounts of defects of the 15 kGy/h and 4 kGy/h experiments, the effect of dose rate in the efficiency in generating defects has been verified, although the concentrations are of the same order of magnitude. Although the amount of F-centre is one order of magnitude lower at 4 kGy/h for samples irradiated at doses below 2 MGy, at higher doses it is similar for both dose rates. In contrast, for colloidal sodium a slightly higher efficiency (2 or 3 times higher) at 4 kGy/h can be observed for the whole range of studied doses.

3.5 Microstructural observations

Microstructural observations were performed on samples from the GIF B-1 and GIF B-2 experiments with a transmitted light polarizing microscope. No microstructural changes were observed on samples of 20 kGy althought radiation induced defects (mainly F-centres) were generated. At doses between 110 and 430 kGy, samples show some light blue areas heterogenously distributed, which have colloidal sodium concentrations around $1.0 * 10^{-6}$ molar fraction. Nevertheless, it was observed that in rock salt having only hyaline halite grains (e.g. SP-800), the faintly blue areas are preferently related to the small grains, while the big grains remain uncoloured. At this dose range, which would represent the induction phase of radiation damage, not pressurized samples (brown-yellow colouration) exhibit higher amounts of F-centre and lower amounts of colloidal sodium than pressurized samples (pale blue colouration).

At doses ranging from 1.1 to 48 MGy, samples are dark blue decorated, having at least colloidal sodium concentrations of 10^{-5} molar fraction. Pressure enhances the generation of radiation induced defects at doses up to 5 MGy. Pressurized samples have between 1.5 and 2 times more sodium colloids than not pressurized, being F-centre concentration not affected by pressure. At doses between 5 and 48 MGy the effect of pressure in defect generation is unnoticeable.

Several microstructural features were visible because of difference in colouration, at doses higher than 1 MGy. These features mainly consist on: white colouration of subgrain boundary microstructures as well as white halos around fluid inclusions and polyhalite crystals, which are similar to those described by Urai et al. (1987), Holdoway (1974) and García Celma et al. (1988) respectively. The aforementioned features can represent an

important bleached zones, provided they are localized in certain grains.

The effect of fluid assisted recrystallization in the form of newly precipitated white halite crystals has also been observed in samples irradiated at doses higher than 1 MGy. These white crystals, free of damage, are the result of grain boundary migration asisted by fluids (García Celma et al. 1988). Solid impurities are rarely found around these white grains, which may act as physical barriers between the colloidal sodium and brine, thus hindering the dissolution-precipitation of halite. These new salt grains commonly contain biphasic fluid inclusions (gas and brine) as well as small rounded inclusions of hydrogen (2-3 μm in size). These grains tend also to grow by preserving at least two cubic faces of slow growth. In general, pressure enhances the neoprecipitation of halite.

In samples where high amounts of newly precipiteted halite were present (e.g. those irradiated under pressure at doses of 44 MGy and dose rate of 4 kGy/h; see figure 11), O.A spectra on white halite areas were performed. The spectra revealed that in those crystals no radiation-induced defects was present. This fact supports the hypothesis that precipitation of halite took place after irradiation stop and might be related either to the temperature decay (from 100ºC to room temperature) and/or to the depressurization of the samples.

In the aforementioned samples, white halite grains were hand picked and high contents of H_2 (equivalent to $2 * 10^{-4}$ molar fraction of colloidal sodium) were measured. Blue halite grains of the same samples have colloidal sodium contents around $5 * 10^{-4}$ molar fraction. Since in the white halite crystals no radiation induced defects were detected, the measured H_2 has to be present as hydrogen inclusions. This H_2 comes from the reaction between colloidal sodium and water, indicating that the grain boundary of new salt grains migrated at the expense of former damaged rock salt, which had at least a molar fraction of colloidal sodium of $2 * 10^{-4}$. Since the measured amounts of H_2 in those samples is similar for the blue and white halite grains it can be concluded that most of the H_2 generated by the reaction of metallic sodium with brine is trapped in the neoprecipitated rock salt.

Quantification of the white halite fraction and the solid impurity content has also been performed. For samples having impuritiy contents higher than 2 %, the amount of white halite is below 1.5 % and usually related to subgrain boundary microstructures, and to the presence of white halos around fluid inclusions and polyhalite crystals. Nevertheless, for purer rock salt high amounts (up to 60 %) of white halite due to fluid assisted recrystallization has been measured (Figure 12). This means that this process may involve a substantial volume of the rock, wiping out the former accumulated defects.

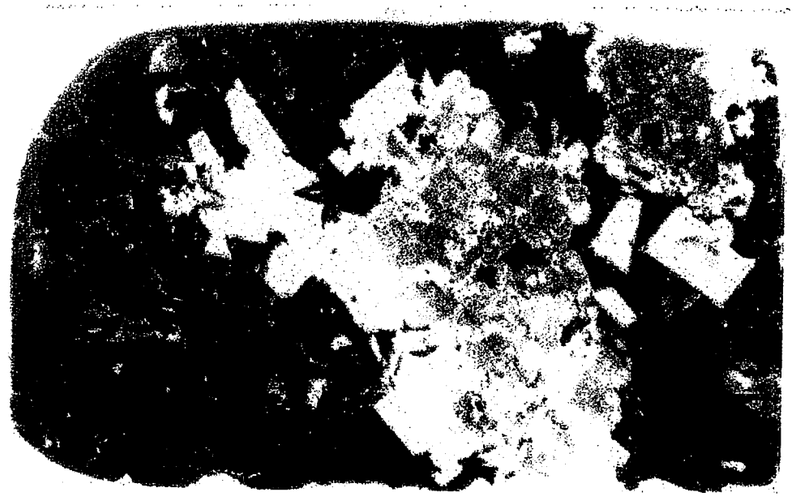

Figure 11: Transmitted light micrograph of the pressurized sample 40PLL irradiated to a dose of 44 MGy (dose rate 4 kGy/h). More than a half of the sample is represented by big crystals of new precipitated halite which tend to develope cubic faces. Long axis of the micrograph is 4 cm.

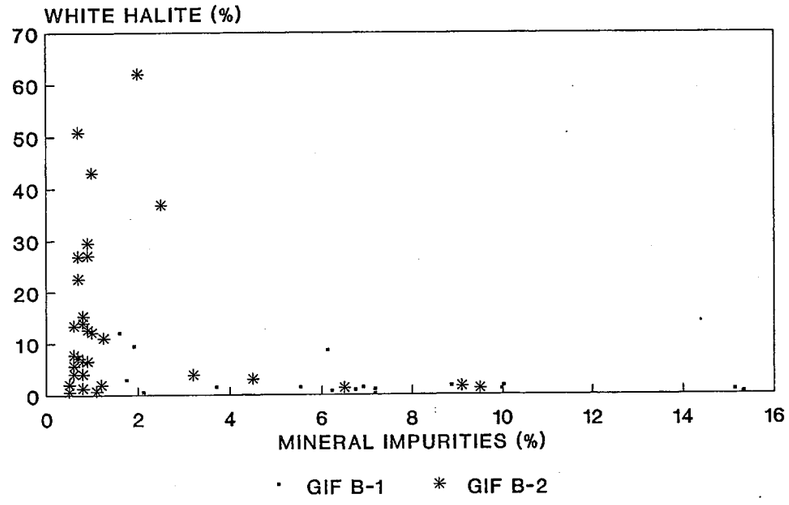

Figure 12: New precipitated white halite versus solid impurity content in irradiated rock salt.

3.6 Factors effecting the formation of radiation induced defects

In order to explain the relationships between the radiation-induced defects and the geological parameters, several Principal Component Analyses (PCA) using the correlation matrix were performed with the data from the GIF B-1 and GIF B-2 experiments. PCA is a statistical multivariate technique (Factor Analysis) which aims to explain the variability of a data set in terms of as few components (factors) as possible. The variables taken into account were: total dose, molar fraction of F-centre, molar fraction of colloidal sodium, size of colloids, confining pressure, as well as the amount of intergranular brine, and the contents of NaCl, SO_4, insoluble fraction, Ca, K, Mg and Sr.

The influence of total dose, confining pressure and brine content in the generation of colloidal sodium was checked in all the cylindrical samples (natural and synthetic). Six input variables were used in the analysis: total dose, molar fraction of F-centre, molar fraction of colloidal sodium, size of colloids, confining pressure and intergranular water content. The results of the Principal Component Analysis performed on samples from the GIF B-1 experiment are listed in Table 1. Similar results have been obtained for the samples of the GIF B-2 experiment.

The first component, which accounts for 50% of total variance, basically weights the contribution of total dose, and the amount of colloidal sodium and size of colloids, with intermediate loadings for the F-centres. Therefore the radiation-induced defects (molar fraction of F-centre, molar fraction of colloidal sodium and size of colloids) are the main parameter related to total dose. The contribution of intergranular water and confining pressure is negligible in this first component. The second and third components are not relevant in this context, reflecting respectively amount of water and pressurization.

The effect of pressure has been studied more in detail, by analyzing its effect in rock samples irradiated to the same total dose. Pressure has its influence in samples irradiated at doses up to 5 MGy, where pressurized samples exhibit more radiation induced defects than non pressurized samples. At higher doses the effect of pressure is negligible.

The influence of accesory minerals and trace elements in the radiation damage has also been analysed in a similar way. Thirteen input variables were used in the analysis: total dose, molar fraction of F-centre, molar fraction of colloidal sodium, size of colloids, confining pressure, and the contents in intergranular water, NaCl, SO_4, insoluble fraction, Ca, K, Mg and Sr. The results of the analysis performed on samples irradiated at the GIF B-1

Table 1: Composition of the first three Eigenvectors (Components) extracted from a data matrix of 6 variables and 84 irradiated rock salt samples in the GIF B-1 experiment.

	COMPONENT 1	COMPONENT 2	COMPONENT 3
DOSE	0.94	-0.09	-0.01
F CENTER	0.69	0.21	-0.14
PRESSURE	0.12	0.61	0.78
SIZE COL.	0.92	-0.16	0.01
COL. NA	0.85	-0.07	0.08
IG. BRINE	0.10	0.79	-0.55
TOTAL VARIANCE	50.0 %	18.0 %	15.8 %

Table 2: Composition of the first three Eigenvectors (Components) extracted from a data matrix of 13 variables and 61 irradiated natural rock salt samples in the GIF B-1 experiment.

	COMPONENT 1	COMPONENT 2	COMPONENT 3
DOSE	0.67	-0.67	0.13
F CENTER	0.65	-0.31	0.38
PRESSURE	0.24	-0.01	0.14
SIZE COL.	0.69	-0.60	0.15
COL. NA	0.68	-0.63	0.18
IG. BRINE	0.04	0.20	0.36
NACL	-0.81	-0.48	0.12
S04	0.75	0.54	0.22
INSOLUBLE	0.72	0.35	-0.34
CA	0.58	0.47	0.38
K	0.51	-0.05	-0.80
MG	0.45	-0.07	-0.74
SR	0.38	0.57	0.22
TOTAL VARIANCE	35.6 %	20.0 %	15.1 %

experiment (dose rate of 15 kGy/h) are listed in Table 2. Similar results have been obtained for the samples of the GIF B-2 experiment (dose rate of 4 kGy/h).

For the first component, which accounts for 36% of total variance, radiation damage shares positive loadings with dose and impurity content. NaCl has negative loadings in this component. The second and third components are not relevant in the context of radiation damage, since they show the presence of celestite and the absence of polyhalite in the studied samples respectively. Since the chemical data reflect the mineralogical composition of the sample, the results of PCA show the influence of the amount of mineral impurities in the rock salt in the formation of radiation induced defects. Similar results have been obtained in a subset of natural non bearing polyhalite rock salt (PLL and BHA), since the presence of polyhalite as mineral impurity enhances the content of K and Mg interstitial ions.

4. DISCUSSION

4.1 Maximal expected damage at the repository

In order to use the experimental results for modelling or prediction at a real repository, one must be aware of the existence of uncertainties which arise from the limited understanding of the radiation damage process. The experimental data have shown the amount of radiation defects is strongly dose dependent. At doses below 10 MGy F-related centres, and one size of colloidal sodium particles are present. At doses between 10 and 50 MGy a second population of colloidal sodium may be present. At doses higher than 100 MGy colloidal sodium particles of sizes ranging between 2 and 150 nm are present.

In all the experiments there is a log-linearity of the amount of radiation induced defects vs. total dose. After reaching a dose of 300 MGy, a decreasing efficiency in generating defects is observed. In the range between 20 and 50 MGy, where the amount of defects has been measured for three diferent dose rates, a change in the efficiency in generating defects has been noted, although their concentration are of the same order of magnitude. Variable dose rate samples (GIF A-2) show 2 times less quantity of defects with regard to the ones of the 15 kGy/h irradiation (GIF B-1), which are also lower (2 or 3 times) with respect to the ones of the 4 kGy/h irradiation (GIF B-2).

An extrapolation of the experimental data with relative high dose rate and temperature of 100 °C to those to be present at a real repository after the first few hundred years (dose rates of 0.1 kGy/h, and probably higher temperatures) should be handled with caution. In addition, the amount of the defects is also governed by the composition of the rock salt, and can vary on one order of magnitude for the same absorbed dose. The effect of recrystallization, which in real repository would have more time to develop, and the fact that we could not observe the effect of back reactions at the early stage could give an erroneus idea of the understanding of the radiation damage process.

Despite these constraints, and since from the available laboratory measurements a probability density function could be defined, in the experiments GIF B-1 and GIF B-2 a probabilistic approach appeared to be the most suitable method for determining the damage which could be expected under these conditions in a repository. The Tchebychev theorem was used to compute the confidence interval for each dose, following the PAGIS methodology (Storck *et al.*, 1988), since the distribution of the amount of defects does not follow a gaussian curve.

The results of the analysis performed on both F-centres and colloidal sodium amount are summarised in Table 3 for the GIF B-1 experiment and in Table 4 for the GIF B-2 experiment. In each table the 50th percentile risk (mean value) and the 95th percentile risk for each total dose are listed. According to Bergsma *et al.*, (1985) and depending on several disposal strategies, the maximum dose for a 0.5 cm thick region in contact with the container over a 100,000 year period would range between 250 and 400 MGy. The different total doses would depend on specific waste parameters such as container diameter, container thickness and temperature. In both cases (GIF B-1 and GIF B-2 experiments), for F-centre the 95th percentile risk varies between 10^{-5} and 10^{-4}. The extrapolation of these data to doses up to 400 MGy, leads us to expect the maximum value of F-centres around 10^{-4}. For colloidal sodium, also in both experiments, the 95th percentile risk follows a quasilinear trend ranging between 10^{-6} and 10^{-3}. The extrapolation to doses up to 400 MGy leads us to expect a maximum value of colloidal sodium below 1 %.

4.2 Comparison between experimental data with the Jain Lidiard model

The results obtained in terms of 50th and 95th percentile for both F-centre and colloidal sodium were compared with the values obtained with the extended version developed by Groote and Weerkamp (1990) of the Jain-Lidiard model. The results are plotted in figures 13 and 14 for the GIF B-1 experiment and in figures 15 and 16 for the GIF B-2

Table 3: Expected concentrations of F-centre and colloidal sodium for several doses (50th and 95th Percentile) for the GIF B-1 experiment.

DOSE	F-CENTER		COLLOIDAL SODIUM	
(MGy)	50TH PC	95TH PC	50TH PC	95TH PC
0.02	1.1E-5	2.2E-5	3.1E-7	6.3E-7
0.23	4.5E-6	9.6E-6	1.6E-6	4.3E-6
0.26	1.4E-5	1.5E-5	1.0E-6	1.9E-6
0.42	1.1E-5	2.1E-5	4.1E-6	8.9E-6
2.61	5.7E-6	1.1E-5	2.6E-5	5.1E-5
3.91	1.3E-5	2.8E-5	3.5E-5	6.1E-5
5.47	2.3E-5	4.3E-5	7.2E-5	1.4E-4
6.95	2.1E-5	3.7E-5	9.3E-5	1.4E-4
16.00	4.8E-5	8.7E-5	2.0E-4	3.8E-4
24.00	3.4E-5	5.0E-5	1.8E-4	2.6E-4
44.65	5.3E-5	8.3E-5	3.2E-4	4.9E-4

Table 4: Expected concentration of F-centre and colloidal sodium for several doses (50th and 95th Percentile) for the GIF B-2 experiment.

DOSE	F-CENTER		COLLOIDAL SODIUM	
(MGy)	50TH PC	95TH PC	50TH PC	95TH PC
0.02	2.5E-6	4.7E-6	9.6E-7	1.7E-6
0.10	1.7E-6	2.7E-6	2.6E-6	4.2E-6
0.21	1.5E-6	3.8E-6	4.1E-6	7.0E-6
0.44	2.3E-6	4.3E-6	1.2E-5	2.1E-5
1.10	6.0E-6	1.2E-5	3.0E-5	5.4E-5
2.22	7.6E-6	1.3E-5	5.6E-5	1.0E-4
4.60	2.3E-5	4.0E-5	6.7E-5	1.9E-4
10.66	3.0E-5	5.7E-5	2.0E-4	3.6E-4
22.70	1.9E-5	4.7E-5	1.1E-4	2.5E-4
44.01	3.4E-5	6.4E-5	2.7E-4	5.6E-4

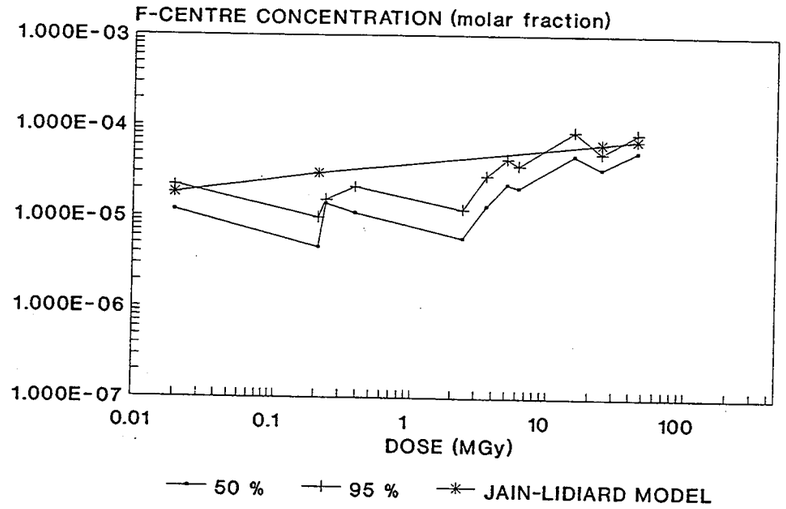

Figure 13: Comparison of the expected concentration of F-centre (50th and 95th Percentile) and the Jain-Lidiard simulation for several doses in the GIF B-1 experiment.

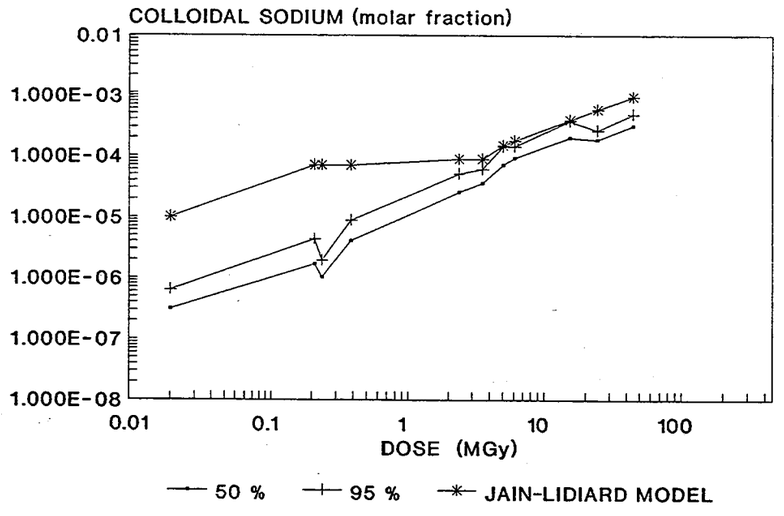

Figure 14: Comparison of the expected colloidal sodium concentration (50th and 95th Percentile) and the Jain-Lidiard simulation for several doses in the GIF B-1 experiment.

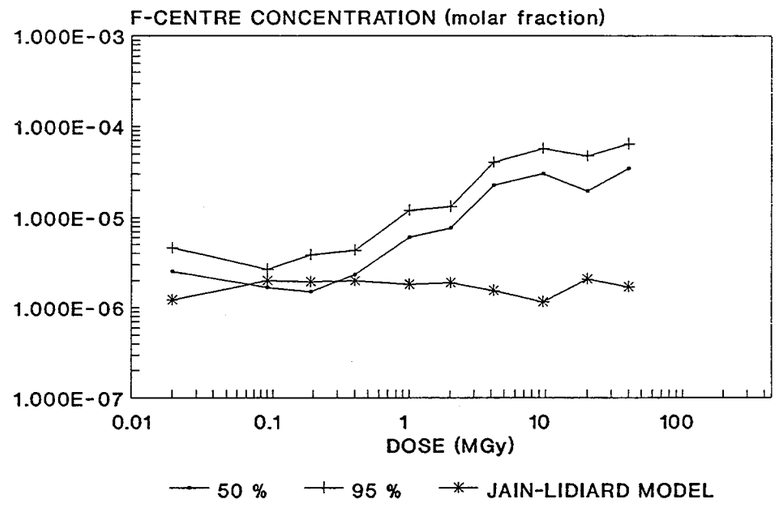

Figure 15: Comparison of the expected F-centre concentration (50th and 95th Percentile) and the Jain-Lidiard simulation for several doses in the GIF B-2 experiment.

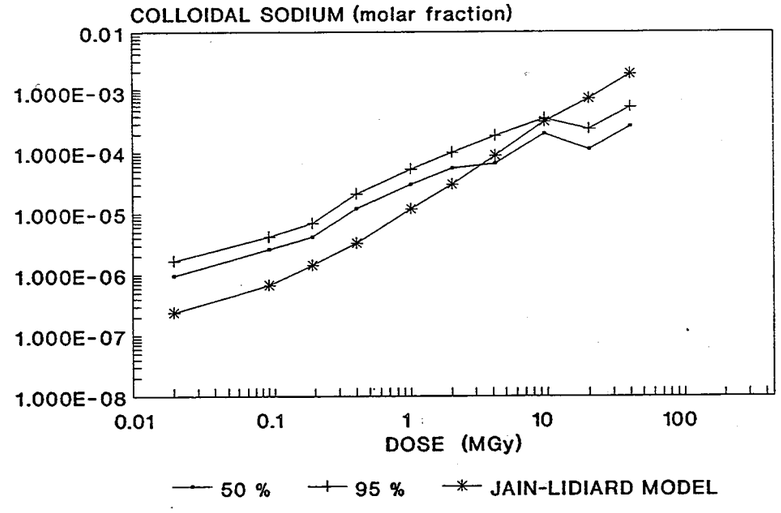

Figure 16: Comparison of the expected colloidal sodium concentration (50th and 95th Percentile) and the Jain-Lidiard simulation for several doses in the GIF B-2 experiment.

experiment respectively.

For the samples irradiated at a dose rate of 15 kGy/h, the 95th percentile of the measured F-centre is of the same order of magnitude than predicted by the Jain-Lidiard simulation. For colloidal sodium, at low doses (smaller than 3 MGy) the Jain Lidiard simulation gives values of one order of magnitude higher than the 95th percentile, while in contrast at higher doses both values tend to converge. However, it is worth noting that the simulation still gives higher values than the 95th percentile risk.

For the samples irradiated at a dose rate of 4 kGy/h, at doses up to 500 kGy, the 50th percentile of the measured F-centre is similar to the predictions of the Jain-Lidiard simulation. At higher doses, the 50th percentile of the measured F-centre is between one and two orders of magnitude higher than the Jain-Lidiard simulation. For colloidal sodium, at low doses (smaller than 2 MGy) the Jain Lidiard simulation gives values of an order of magnitude lower than the 95th percentile, while in contrast at higher doses both values tend to converge. At doses of 22 and 44 MGy, the simulation gives higher values than the 95th percentile which is explained by the extensive recristallization phenomena.

The obtained results focus that reliable predictions on the generation of colloidal sodium for doses higher than 5 MGy, can be obtained with this version of the Jain-Lidiard model. In contrast, F-centres are not accurately predicted. Nevertheless, and regarding safety relevant aspects of radiation damage, this model has proven its efficacy for the dose rates and temperatures used in the experiments. However, it should be further validated at other temperatures and realistic dose rates.

5. CONCLUSIONS

Laboratory irradiations at a temperature of 100ºC and several dose rates (variable dose rate between 200 and 20 kGy/h and constant dose rates of 15 and 4 kGy/h) have enabled the study of the radiation damage on several types of rock salt. The analyses take into account the concentration of radiation-induced defects in relation with dose, dose rate and the geological characteristics of the host rock.

In general, there is a good correlation between the two methods of determining radiation damage, yielding results of the same order of magnitude, except for samples irradiated at doses higher than 100 MGy. In those samples, and due to the complexity of the Optical absorption spectra, hydrogen measurements give a better resolution. Hydrogen

measurements are a very fast method of determining the colloidal sodium amount, but do not quantify other colour centres developed by irradiation. In contrast, Optical absorption is very time consuming.

The amount of F-centres as well as the amount of colloidal sodium increases log-linerily with increasing total dose. The concentration of colloidal sodium is very sensitive to the absorbed dose at doses up to 300 MGy. At higher doses (up to 1154 MGy) a decreasing efficiency in generating colloidal sodium particles is observed. The amount of F-centres increases not so sensitively reaching the steady state at a molar fraction of $4 * 10^{-4}$.

Another notable trend is that colloidal particle size grows with increasing dose. In samples irradiated at doses higher than 10 MGy, two populations of colloids may coexist: small colloids (about 5 nm diameter) and large colloids (between 80 and 90 nm diameter). At doses higher than 100 MGy, after reaching a colloidal sodium concentration of 10^{-3} the size of the particles ranges between 2 and 150 nm.

Comparing radiation damage between pure monocrystals and natural rock salt, the radiation damage in monocrystals is one order of magnitude less than in rock salt. This fact is explained by the low dislocation and impurity concentration of pure monocrystals and therefore they can not easily nucleate colloids. Despite its lower amount of colloidal sodium particles, their size is around 90 nm independently on the absorbed dose.

The effect of dose rate is also responsible of variations in the amount of defects for samples irradiated at the same total dose. Low dose rates shows a slightly higher efficiency in generating defects, althought their concentrations are of the same order of magnitude.

For samples of the same type and irradiation conditions the amount of measured defects is widely scattered (on one order of magnitude). Geochemical parameter intrinsic of the rock salt are more important in the generation of the radiation induced defects than the effect of the different studied dose rates. The mineralogical impurity of the rock salt enhances the development of radiation induced defects. Therefore, mineralogically pure rock salt formations may be more suitable to host radiactive waste than impure rock salt. This information can be very helpful in site characterization. In contrast, the influence of brine content in radiation damage is weak.

White halite (free of radiation induced defects) formed by grain boundary migration assisted by fluids has been extensively recognized in natural rock salt from GIF B-1 and GIF B-2 experiments. This process can be very important in pressurized and pure samples (halite content higher than 98 %). These white crystals commonly contain small hydrogen inclusions. Hidrogen is the product of the reaction between former halite grains, which had already developed colloids and intergranular brine. The major part of the H_2 generated in the reaction is trapped in the neoprecipitated halite, giving smaller releases of H_2 than expected in the repository. Since no radiation induced defects were detected in the white halite it has to be concluded that grain boundary migration took place after irradiation stop and therefore related to temperature and/or pressure decay.

It should be taken into account that for doses higher than 5 MGy, the amount of colloidal sodium obtained by the Jain-Lidiard simulation are slightly higher than the 95th percentile of risk based on the experimental results. However, extrapolations to repository conditions should be made after performing irradiation experiments at doses up to 5-10 MGy with realistic dose rate and temperature, in order to asssure that the emplacement of waste will not threaten the long-term safety of the repository.

ACKNOWLEDGEMENTS

The work reported here has been performed on behalf of ENRESA under contract No 70.2.3.13.03. We are indebted to Mr. J.M. Grosso and Ms. P. Teixidor from the LIFS for their assisstance at the laboratory. We make extensive our recognition to Dr. X. Dies of the Dept. d' Enginyería Nuclear de la Universitat Politècnica de Catalunya (UPC), who kindly performed the Jain-Lidiard simulations.

6. REFERENCES

BERGSMA, J., HELMHOLDT, R.B. and HEIJBOER, R.J, 1985: *"Radiation dose deposition and colloid formation in a rock salt waste repository"*, Nucl. Technology, **71**, 597-607

DALE COMPTON, W., 1957: *"Production of colloidal sodium in NaCl by ionizing radiation"*, Phys.Rev., **107**, 1271-1276

HOLDOWAY, K.A., 1974: *"Behaviour of fluid inclusions in salt during heating and irradiation"* in "Fourth Symp. on Salt. North. Ohio Geol. Soc.", 303-312

GARCIA CELMA, A., URAI, J.L. and SPIERS, C.J., 1988: *"A laboratory investigation into the interaction of recrystallization and radiation damage effects in polycrystalline salt rocks"*, Nuclear Science and Technology, EUR 11849 EN, 125p

GROOTE, J. and WEERKAMP, H.R., 1990: *"Radiation damage in NaCl; small particles"*, Ph.D. Thesis, Univ.Groningen, 270p

HODGSON, E.R., DELGADO, G. and ALVAREZ RIVAS, J.L., 1979: *"In-beam studies of M-centre production processes in NaCl"*, Jour.Phys. C: Sol.Sta.Phys., **12**, 1239-1244

HUERTAS, F., MAYOR, J.C. and DEL OLMO, C., 1992: *"Textural and Fluid Phase Analysis of Rock Salt subjected to the combined effects of Pressure, Heat and Gamma Radiation"*, Nuclear Science and Technology, EUR 14169 EN, 218p

IKEDA, T. and YOSHIDA, S., 1967: *"Effect of divalent cation impurities on the formation and bleaching of colloids in NaCl"*, Jour.Phys.Soc.Jap., **22**, 138-143

JAIN, U. and LIDIARD, A.B., 1977: *"The growth of colloidal centres in irradiated alkali halides"*, Phil.Mag., **35**, 245-259

JENKS, G.H. and BOPP, C.D., 1974: *"Storage and release of radiation energy in salt in radioactive waste repositories"*, ORNL-TM-4449, 77p

JENKS, G.H., SONDER, E., BOPP, C.D., WALTON, J.R. and, LINDEBAUM, S., 1975: *"Reaction products and stored energy released from irradiated sodium chloride by dissolution and by heating"*, Jour. Phys. Chem., **79**, 871-875

LEVY, P.W., 1983: *"Radiation damage on natural rock salt from various geological localities of interest to the radioactive waste disposal program"*, Nucl. Technology, **60**, 231-243

LEVY, P.W. and KIERSTEAD, J.A., 1984: *"Very rough preliminary estimate of the sodium metal colloid induced in natural rock salt by the radiations from radioactive waste canisters"*, Mat.Res.Soc.Symp.Proc., **26**, 727-734

MARKHAM, J.J., 1966: *"F-Centres in Alkali Halides"*. Academic Press Inc. 400p

MÖNIG J., GARCIA CELMA A., HELMHOLDT R.B., HINSCH H. HUERTAS F. and PALUT J.M., 1990: *"The HAW Project: Test disposal of high-level waste in the Asse salt mine. International test-plan for irradiation experiments"*, Nuclear Science and Technology EUR 12946 EN, 76p

PRZIBRAM, K., 1956: *"Irradiation colours and luminiscence; a contribution to mineral physics"*, Pergamon Press, 332p

SCHULZE, O., 1986: *"Der Einfluss radioaktiver Strahlung auf das mechanische Verhalten von Steinsalz"*, Z.dt.geol.Ges., **137**, 47-69

SMITHARD, M.A. and TRAN, M.Q., 1974: *"The optical absorption produced by small sodium metal particles in sodium chloride"*, Helv.Phys.Acta, **46**, 869-888

STORCK, R., ASCHENBACH, J., HIRSEKOM, R.P., NIES, A. and STELTE, N., 1988: *"Performance Assessment of Geological Isolation Systems for Radioactive Waste: Disposal in Salt formation"*, Nuclear Science and Technology, EUR 11778 EN, 788p

URAI, J.L.; SPIERS, C.J.; PEACH, C.J.; FRANSSEN, R.C.M.W. and LIEZENBERG, J.L., 1987: *"Deformation mechanisms operating in naturally deformed halite rocks as deduced from microstructural investigations"*, Geol.Mijn., **66**, 165-176

VAN OPBROEK, G. and DEN HARTOG, H.W., 1985: *"Radiation damage of NaCl: dose rate effects"*, Jour.Phys. C: Sol.Sta.Phys., **18**, 257-268

COLLOID FORMATION AND STORED ENERGY DEPOSITION IN IRRADIATED NATURAL ROCK SALT SAMPLES

J. Mönig, N. Jockwer, H. Gies

ABSTRACT

The temperature dependence of the radiation-induced formation of colloidal sodium, molecular chlorine gas and the associated deposition of energy in rock salt was determined between 100 °C and 250 °C. At each temperature the irradiation dose was varied between 10^6 and 10^8 Gy. After irradiation, the colloidal sodium content was measured via hydrogen evolution upon dissolving the salt in water. The amounts of chlorine gas were determined both in the gas phase above the salt and in the bulk of the sample. Stored energy was determined by DSC on selected halite specimens. The present study confirms the equivalence of the radiation-induced formation of the different products, i.e. colloidal sodium, molecular chlorine, and stored energy, over a substantial dose range and temperature range. The chosen range is of interest for radioactive waste repositories. From the data obtained it is concluded, that at temperatures above 150 °C, colloid formation starts to saturate with increasing dose. At 100 °C about 0.7 mol % sodium were detected for 10^8 Gy but no saturation was indicated. Most of the molecular chlorine is found, after irradiation, inside the salt crystals of the bulk sample, but chlorine evaporation from the salt increases with increasing temperature. The stored energy follows the trends outlined for the molecular radiation products, i.e. it increases with dose. A conversion factor of about 70 J/g per mol % colloidal sodium in the rock salt is found by us. This value is lower than that proposed by Groote and Weerkamp of 125 J/g per mol % colloidal sodium [Groote and Weerkamp, 1990]. The reason for this difference is explained by Donker et al. [Donker et al., 1995 (article nr. 19, this volume)]. They obtained a value for the equivalence of stored energy and colloid content that is much nearer to one obtained by us than to that of Groote and Weerkamp. The influence of sulfate-containing minerals as anhydrite and polyhalite on the formation of radiation damage and stored energy was investigated but the present data do no allow to derive any final conclusion.